

## Spectroscopic and Microstructural Analysis of Phase Transformation of Mg-PSZ/Al<sub>2</sub>O<sub>3</sub> Fibers Prepared by Sol-Gel Method

Hee Tai Eun and Chin Myung Whang

Dept. of Ceramic Eng., and Center for Molecular Dynamics, Inha Univ., Incheon 402-751, Korea  
(Received June 4, 1996)

The Mg-PSZ/Al<sub>2</sub>O<sub>3</sub> fibers were fabricated by the sol-gel method. The added Al<sub>2</sub>O<sub>3</sub> amounts were varied from 5 to 20 mol%. The phase transformation studies of a drawn Mg-PSZ/Al<sub>2</sub>O<sub>3</sub> fibers were investigated by use of X-ray diffraction, IR and Raman spectroscopy. Microstructure and tensile strength of fibers were subjected to scanning electron microscopy and tensile strength tester. When Al<sub>2</sub>O<sub>3</sub> was added to the Mg-PSZ fibers, it was found out from the analysis of XRD patterns and Raman spectra that a small amount of crystalline spinel (MgAl<sub>2</sub>O<sub>4</sub>) started to form due to the reaction between Al<sub>2</sub>O<sub>3</sub> and MgO, at 1000°C, and the phase transformation temperature of ZrO<sub>2</sub> crystal phase at different sintering temperatures increased. Also, the rapid grain growth with average grain size of 2.0 μm shown in Mg-PSZ fiber at 1500°C was considerably suppressed to 0.39 μm by adding Al<sub>2</sub>O<sub>3</sub> at the same temperature. When the Mg-PSZ/Al<sub>2</sub>O<sub>3</sub> fibers containing 5 mol% Al<sub>2</sub>O<sub>3</sub> were sintered at 800°C for 1 hr, average tensile strength of fibers was 0.9 GPa at diameters of 20 to 30 μm, but as the sintering temperatures was increased to 1000°C for 1 hr, average tensile strength of fibers increased to 1.2 GPa in the same diameter range.

**Key words :** Sol-gel method, Mg-PSZ/Al<sub>2</sub>O<sub>3</sub> fibers, IR and Raman spectroscopy

### I. Introduction

Ceramic fibers are considered to be a good candidate for high-temperature applications in composite with metal or ceramic matrices. Stabilized ZrO<sub>2</sub> fibers have attracted much attention because of their high mechanical strength as well as their high refractoriness. Many workers<sup>1-9,13</sup> have been investigated the sol-gel method for preparation of partially stabilized ZrO<sub>2</sub> fibers with various dopants such as MgO, CaO, and Y<sub>2</sub>O<sub>3</sub>. In a previous paper, Whang et al.<sup>9</sup> reported the effect of phase transformation of MgO-ZrO<sub>2</sub> fibers as MgO sources were varied from magnesium nitrate, to acetate, and to ethylate. Also, studies on phase transformation of MgO-ZrO<sub>2</sub> fibers depending on the amount of MgO and heat treatment temperatures were carried out by means of X-ray diffraction and vibrational spectroscopy. The tensile strength of MgO-ZrO<sub>2</sub> fibers were greatly affected by the phase transformation and the microstructure of fibers at various sintering temperature.

According to our results,<sup>9</sup> the tensile strength of the 800°C-sintered MgO-ZrO<sub>2</sub> fibers is about 4.0 GPa at diameter of 20~30 μm, while that of the 1000°C-sintered fibers decreases rapidly to about 0.7 GPa at the same diameter. The factors resulting in the lowering of MgO-ZrO<sub>2</sub> fiber strength were thought to be the loss of transformation toughening from tetragonal to monoclinic transformation, grain growth, and residual pores. These factors were confirmed through XRD, IR, Raman, SEM, and micropore measurement.

Recently, to improve the high temperature strength of ZrO<sub>2</sub> fibers, several researchers have tried to prepare the ZrO<sub>2</sub> composite fibers containing Al<sub>2</sub>O<sub>3</sub> or mullite.<sup>9,10</sup> It has been reported that the addition of Al<sub>2</sub>O<sub>3</sub> increases both room and high temperature strength of Y<sub>2</sub>O<sub>3</sub>-ZrO<sub>2</sub> fiber. The strength of the ZrO<sub>2</sub> composite containing 2 mol% Y<sub>2</sub>O<sub>3</sub> and 40 wt% Al<sub>2</sub>O<sub>3</sub> was found to be 1 GPa at 1000°C, which is nearly four times higher than that of the Al<sub>2</sub>O<sub>3</sub> free Y<sub>2</sub>O<sub>3</sub>-ZrO<sub>2</sub>.<sup>11,12</sup> Sim et al.<sup>13</sup> investigated the effect of the addition of Al<sub>2</sub>O<sub>3</sub> on the microstructure of the ZrO<sub>2</sub> fibers containing 3 mol% Y<sub>2</sub>O<sub>3</sub>. Their results indicated that the presence of the Al<sub>2</sub>O<sub>3</sub> aids densification of the Y<sub>2</sub>O<sub>3</sub>-ZrO<sub>2</sub> fibers. Addition of 5 wt% Al<sub>2</sub>O<sub>3</sub> enhances the ZrO<sub>2</sub> grain growth and the further addition inhibits the ZrO<sub>2</sub> grain growth at 1400°C. Also, as sintering temperature increases, the Al<sub>2</sub>O<sub>3</sub> particles grow with the ZrO<sub>2</sub> grains and become elongated due to the presence of small amount of intergranular amorphous phase.

Diffusion processes and solid state reactions between Al<sub>2</sub>O<sub>3</sub> and stabilized ZrO<sub>2</sub> containing Y<sub>2</sub>O<sub>3</sub>, CaO, and MgO in solid solutions have been reported to display quite different behaviors. Kosmac et al.<sup>14</sup> concluded that, in the systems Al<sub>2</sub>O<sub>3</sub>-ZrO<sub>2</sub>-CaO and Al<sub>2</sub>O<sub>3</sub>-ZrO<sub>2</sub>-MgO, the stabilizing oxides react with Al<sub>2</sub>O<sub>3</sub> resulting in the formation of Ca aluminates and Mg-Al spinel, respectively. In the system Al<sub>2</sub>O<sub>3</sub>-ZrO<sub>2</sub>-Y<sub>2</sub>O<sub>3</sub>, diffusion of Y<sub>2</sub>O<sub>3</sub> into Al<sub>2</sub>O<sub>3</sub> does not take place. It is interesting to find out whether the same kind of destabilization of ZrO<sub>2</sub> would be observed in the Mg-PSZ/Al<sub>2</sub>O<sub>3</sub> fiber resulting in formation of MgAl<sub>2</sub>O<sub>4</sub> spinel.

The object of the present study is to prepare the MgO-ZrO<sub>2</sub>-Al<sub>2</sub>O<sub>3</sub> fibers and to find out the effect of the Al<sub>2</sub>O<sub>3</sub> addition on phase transformation containing 12 mol% MgO(Mg-PSZ/Al<sub>2</sub>O<sub>3</sub>). Studies on crystalline phase and phase transformation of Mg-PSZ/Al<sub>2</sub>O<sub>3</sub> fibers depending on the amount of Al<sub>2</sub>O<sub>3</sub> and sintering temperatures have been investigated by means of XRD and vibrational spectroscopy. Also, stability of MgO-doped ZrO<sub>2</sub> fiber in the presence of Al<sub>2</sub>O<sub>3</sub> has been examined.

Additionally, we have investigated and measured the microstructure and the tensile strength of Mg-PSZ/Al<sub>2</sub>O<sub>3</sub> fibers through SEM and fiber tensile strength tester, respectively.

## II. Experimental Procedure

### 1. Preparation of Mg-PSZ/Al<sub>2</sub>O<sub>3</sub> fibers

In the preparation of Mg-PSZ/Al<sub>2</sub>O<sub>3</sub> fibers by sol-gel method, Zr(O-nC<sub>3</sub>H<sub>7</sub>)<sub>4</sub>, Mg(NO<sub>3</sub>)<sub>2</sub>·6H<sub>2</sub>O, and AlCl<sub>3</sub> were used as starting materials. The amount of MgO was fixed at 12 mol% and that of Al<sub>2</sub>O<sub>3</sub> was varied from 5 to 20 mol%

The Mg-PSZ/Al<sub>2</sub>O<sub>3</sub> fibers were fabricated according to the flow chart shown in figure 1. Initially, 1.2 M Zr(O-nC<sub>3</sub>H<sub>7</sub>)<sub>4</sub>-C<sub>2</sub>H<sub>5</sub>OH solutions were weighed in glove box under N<sub>2</sub> atmosphere and stirred in a waterbath at 25°C for 1 hr. The other mixed solution of Mg(NO<sub>3</sub>)<sub>2</sub>·6H<sub>2</sub>O-AlCl<sub>3</sub>-C<sub>2</sub>H<sub>5</sub>OH-HNO<sub>3</sub> was added dropwise to the Zr(O-nC<sub>3</sub>H<sub>7</sub>)<sub>4</sub>-C<sub>2</sub>H<sub>5</sub>OH solution using a syringe. The prepared sol solutions were concentrated at 80°C using a waterbath until they became viscous and sticky. When the sol solution was

concentrated enough for fiber drawing, the ZrO<sub>2</sub> gel fibers were drawn by immersing a glass rod and pulling it up by hand in the laboratory under 60% humidity at 25°C. The drawn gel fibers were dried for 24 hrs at the same conditions in the same place, and sintered in ambient air at various temperatures.

### 2. Measurements

To investigate the crystalline phase and phase transformation of drawn Mg-PSZ/Al<sub>2</sub>O<sub>3</sub> fibers depending on the amount of Al<sub>2</sub>O<sub>3</sub> and sintering temperature, the Mg-PSZ/Al<sub>2</sub>O<sub>3</sub> fibers were heated at various temperatures and identified by means of X-ray diffractometer (Philips Co., PW 3020), Fourier Transform Infrared (Bio-Rad Co., FTS 165), and Raman spectrometer (Spex Co., RAMALOG 101).

The X-ray diffraction measurement conditions were Ni-filtered CuKα radiation, 45 kV, 40 mA, scanning range of 20°~80°[2θ], and scanning speed of 0.04° (2θ/sec). A small amount of pulverized ZrO<sub>2</sub> fibers was mixed with KBr powder and pressed into a transparent pellet. The mid-infrared spectra of the sample were recorded from 400~1000 cm<sup>-1</sup> with a resolution of 2 cm<sup>-1</sup> equipped with a KBr beam splitter. The macro-Raman spectra of the pulverized fibers were recorded in the frequency of 80~800 cm<sup>-1</sup> using the 514.5 nm line of an Argon ion laser as an excitation source.

Thermal properties of drawn gel fibers were investigated in ambient air at a heating rate of 5°C/min using DT/TG analyzer (TA Instrument Co., SDT 1500).

The microstructure of the fibers depending on the Al<sub>2</sub>O<sub>3</sub> content and the sintering temperature was observed through SEM (Hitachi Co., X-650). The tensile strength of the fibers was measured using fiber tensile strength tester made in the laboratory.

## III. Results and Discussion

We fabricated the Mg-PSZ/Al<sub>2</sub>O<sub>3</sub> fibers at the optimum experimental conditions, H<sub>2</sub>O/alkoxide molar ratio of 3~4, HNO<sub>3</sub>/alkoxide molar ratio of 1.3~1.5, initial pH of 0.6 and the total molar ratio of ethanol of 21.6, as reported in the previous study.<sup>8)</sup>

When the sol solutions were concentrated for 5~6 hrs in a waterbath maintained at 80°C, all of the gel fibers could be drawn by using a glass rod. The viscosity of sol solutions was about 20 Poise.

### 1. X-ray diffraction

Figure 2 shows X-ray diffraction patterns of Mg-PSZ/Al<sub>2</sub>O<sub>3</sub> fibers at 1500°C when the Al<sub>2</sub>O<sub>3</sub> content was varied from 0 to 20 mol%. Cubic and monoclinic peaks coexist in the Al<sub>2</sub>O<sub>3</sub> free fibers as shown in the previous work,<sup>8)</sup> and at 5 mol% Al<sub>2</sub>O<sub>3</sub> the intensity of the cubic peak decreases considerably while that of the monoclinic peaks increases. As the amount of Al<sub>2</sub>O<sub>3</sub> increases up to 20 mol%, the phase transforms completely to monoclinic. In the previous

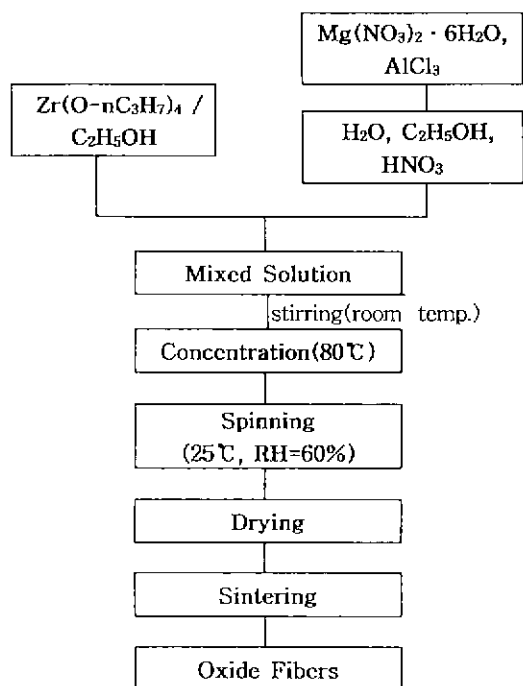
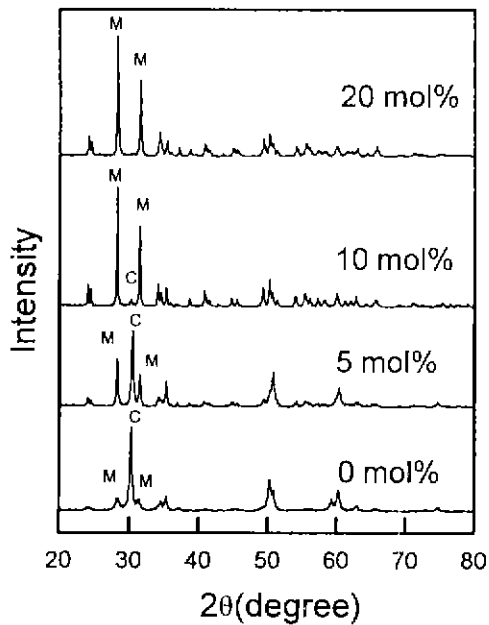


Fig. 1. Flow chart for preparing Mg-PSZ/Al<sub>2</sub>O<sub>3</sub> fibers through sol-gel process.



**Fig. 2.** X-ray diffraction patterns of 12Mg-PSZ/Al<sub>2</sub>O<sub>3</sub> fibers sintered at 1500°C for 1 hr taken as a function of Al<sub>2</sub>O<sub>3</sub> amount [M: Monoclinic, C: Cubic].

study,<sup>14</sup> it was shown that Y<sub>2</sub>O<sub>3</sub>-stabilized ZrO<sub>2</sub>(YSZ) cannot be substantially destabilized by Al<sub>2</sub>O<sub>3</sub>. On the other hand, CaO-stabilized or MgO-stabilized ZrO<sub>2</sub> reacts with Al<sub>2</sub>O<sub>3</sub>, resulting in the formation of Ca aluminates and Mg-Al spinel, respectively.

To investigate the formation of spinel in more details, we were subjected to X-ray analysis of sintered Mg-PSZ/Al<sub>2</sub>O<sub>3</sub> fibers as a function of Al<sub>2</sub>O<sub>3</sub> amount at 1500°C in the range of 34°~50°(2θ) as shown in figure 3. This result confirmed the fact that MgO react with Al<sub>2</sub>O<sub>3</sub>, resulting in the formation of spinel (MgAl<sub>2</sub>O<sub>4</sub>). The spinel peak intensity increases with the increment of Al<sub>2</sub>O<sub>3</sub> content. On the other hand, in the system of stabilized ZrO<sub>2</sub> fibers containing 3 mol% Y<sub>2</sub>O<sub>3</sub> and 15 wt% Al<sub>2</sub>O<sub>3</sub>, well-defined tetragonal ZrO<sub>2</sub> and α-Al<sub>2</sub>O<sub>3</sub> phase existed.<sup>15</sup> It suggested the fact that diffusion of Y<sub>2</sub>O<sub>3</sub> into Al<sub>2</sub>O<sub>3</sub> did not take place and no yttrium aluminates formation occurred. These results are consistent with the previous results reported by Kosmac et al.<sup>14</sup>

Figures 4 and 5 represent the results of phase transformation of 12 mol% Mg-PSZ fibers(12MZ) containing 5 mole% Al<sub>2</sub>O<sub>3</sub>(12MZ5A) and 20 mole% Al<sub>2</sub>O<sub>3</sub>(12MZ20A), respectively, as a function of sintering temperature.

Amorphous phase exists until 400°C. The crystalline species of sintered fibers with two different Al<sub>2</sub>O<sub>3</sub> contents at 800°C were metastable cubic in both cases. However, at 1000°C, the phase of 12MZ5A exists as monoclinic with traces of tetragonal while that of 12MZ 20A exists mainly as tetragonal with a small amount of monoclinic. The crystalline phase changes completely to monoclinic at 1200°C in both cases. As the sintering temperature increases up to 1500°C, monoclinic and cubic

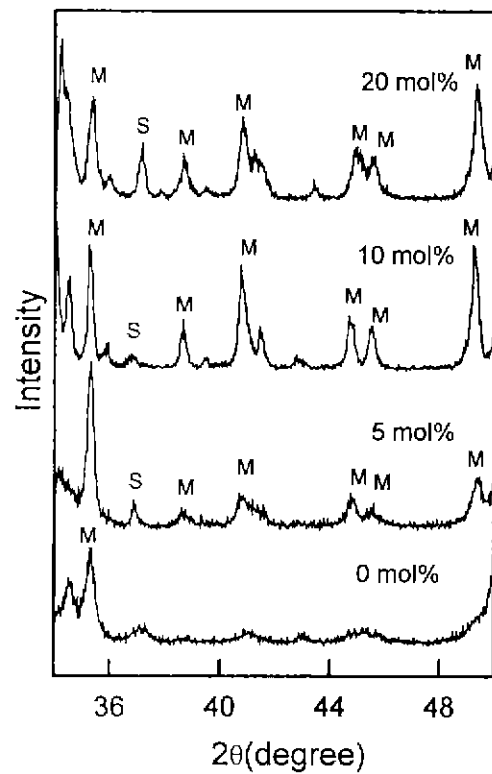


**Fig. 3.** Identification of spinel peaks in XRD patterns of 12Mg-PSZ/Al<sub>2</sub>O<sub>3</sub> fibers sintered at 1500°C for 1 hr taken as a function of Al<sub>2</sub>O<sub>3</sub> amount [M: Monoclinic, S: Spine (MgAl<sub>2</sub>O<sub>4</sub>)].

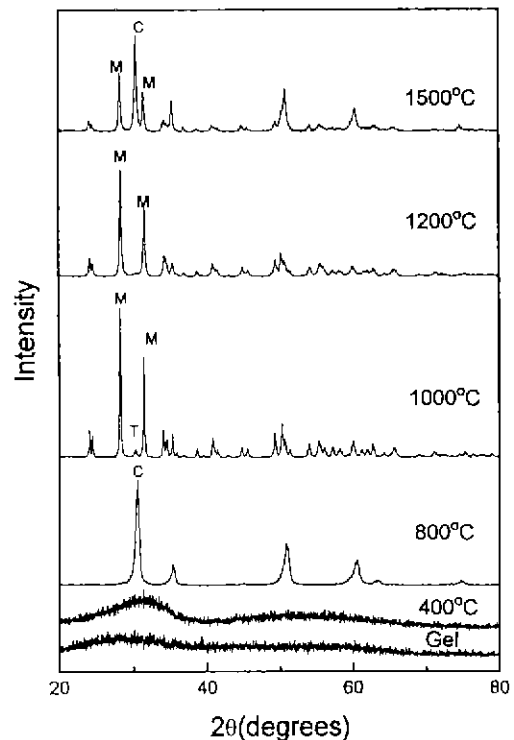


**Fig. 4.** X-ray diffraction patterns of 12Mg-PSZ/5Al<sub>2</sub>O<sub>3</sub> (mol%) fibers sintered at different temperatures for 1 hr [M: Monoclinic, T Tetragonal, C: Cubic].

phase coexist in the case of 12MZ5A while the crystalline phase of 12MZ20A remain monoclinic.

In figure 6 are shown the XRD analyses of the formation of spinel at different sintering temperatures in

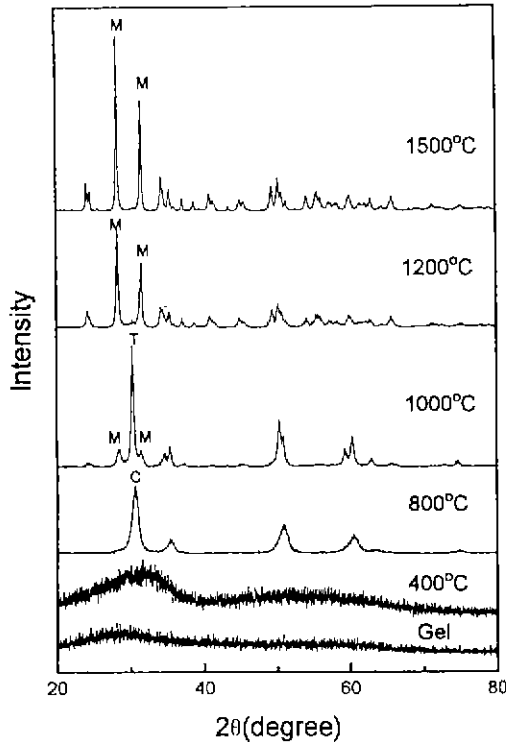
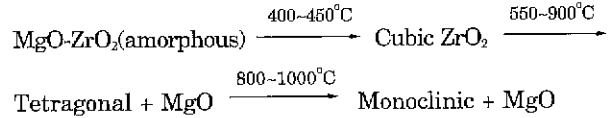


**Fig. 5.** X-ray diffraction patterns of 12Mg-PSZ/20Al<sub>2</sub>O<sub>3</sub>(mol%) fibers sintered at different temperatures for 1 hr [M: Monoclinic, T: Tetragonal, C: Cubic].

the range of 34°~50°(2θ). There are no MgAl<sub>2</sub>O<sub>4</sub> spinel formation for both samples at 800°C. As the sintering temperature increases from 1000 to 1500°C, we can observe the fact that a broad and weak spinel peak become stronger and narrower.

The effect of addition of Al<sub>2</sub>O<sub>3</sub> on the phase transformation of 12MZ fiber is summarized in Table 1.

It has been proposed<sup>15)</sup> that the probable sequence of phase transformations with the thermal evolution of MgO-ZrO<sub>2</sub> amorphous gel containing 3 to 15 mol% MgO can be summarized in the following paths;



As shown in Fig 4, 5, and 6, 12MZ5A and 12MZ20A exist as a single cubic solid solution. As the temperature increases to above 800°C, cubic phase decomposes into tetragonal and MgO. Consequently, diffusion of MgO into the Al<sub>2</sub>O<sub>3</sub> preferentially occurs and MgAl<sub>2</sub>O<sub>4</sub> spinel presumably forms. For sample 12MZ5A, intermediate tetragonal phase transforms to the monoclinic phase at 1000°C in agreement with the results suggested by Kundu et al.<sup>15)</sup>

However, in the case of the sample 12MZ20A, characteristics of tetragonal phase are predominantly exhibited with traces of monoclinic at 1000°C. The retention of tetragonal phase at 1000°C suggests that the further increase of spinel formation for sample 12MZ20A retard the ZrO<sub>2</sub> grain growth.

It has been reported<sup>16)</sup> that tetragonal phase ZrO<sub>2</sub> will

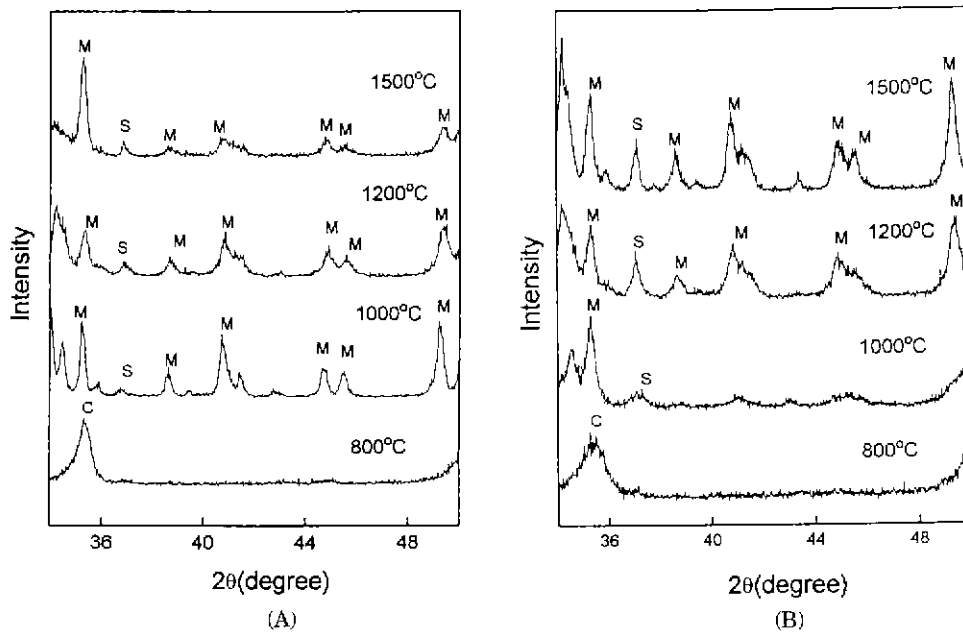


**Fig. 6.** Identification of spinel peaks in XRD patterns of 12Mg-PSZ/Al<sub>2</sub>O<sub>3</sub>(mol%) fibers containing 5 mol% Al<sub>2</sub>O<sub>3</sub>(A) and 20 mol% Al<sub>2</sub>O<sub>3</sub> (B) sintered at different temperatures [C: Cubic, M: Monoclinic, S: Spinel(MgAl<sub>2</sub>O<sub>4</sub>)].

**Table 1.** Crystalline Phases of Mg-PSZ and Mg-PSZ/Al<sub>2</sub>O<sub>3</sub> Fibers at Different Sintering Temperatures

Temperature	12MZ	12MZ5A	12MZ20A
Room Temperature	Amorphous	Amorphous	Amorphous
400°C	Cubic	Amorphous	Amorphous
800°C	Metastable Tetragonal	Metastable Cubic	Metastable Cubic
1000°C	Monoclinic	Monoclinic+Tetragonal+Spinel	Tetragonal+Monoclinic+Spinel
1200°C	Monoclinic	Monoclinic+Spinel	Monoclinic+Spinel
1500°C	Cubic+Monoclinic	Cubic+Monoclinic+Spinel	Monoclinic+Spinel

12MZ: 12 mol% MgO-ZrO<sub>2</sub>.

12MZ5A: 12 mol% MgO-ZrO<sub>2</sub>+5 mol% Al<sub>2</sub>O<sub>3</sub>.

12MZ20A: 12 mol% MgO-ZrO<sub>2</sub>+20 mol% Al<sub>2</sub>O<sub>3</sub>.

Spinel: MgAl<sub>2</sub>O<sub>4</sub>.

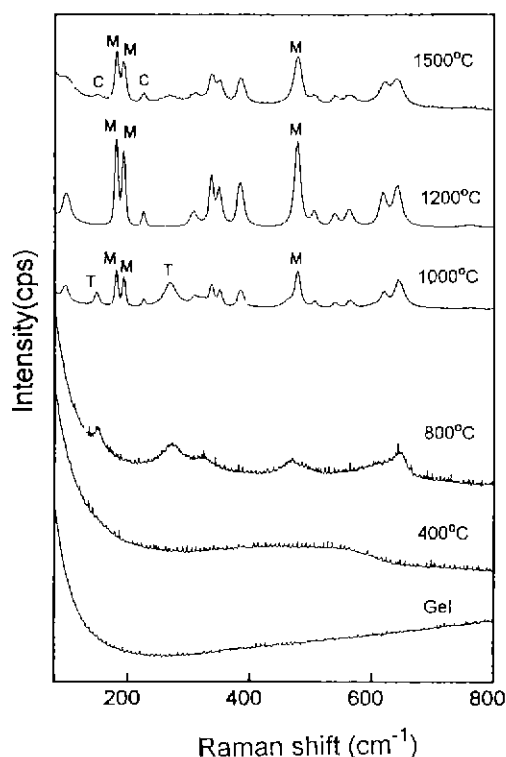


**Fig. 7.** Raman spectra of 12Mg-PSZ/5Al<sub>2</sub>O<sub>3</sub>(mol%) fibers sintered at different temperatures for 1 hr [M: Monoclinic, T: Tetragonal, C: Cubic].

transform to the monoclinic phase spontaneously if the size of the tetragonal phase exceeds a critical value (0.2  $\mu\text{m}$  for MgO-ZrO<sub>2</sub>). When the temperature is raised to 1500°C, monoclinic phase of 12MZ5A converts more easily to the cubic phase than that of 12MZ20A.

## 2. Vibrational study

The length of periodicity for diffraction of X-rays must be near the coherence length, which varies for different sources but is the order of 40 to 100Å. This requirement renders X-rays rather insensitive to structural changes that may occur before such long-range order is attained. On the other hand, Raman spectroscopy is a particularly attractive method for the characterization of materials

such as the phase transformation owing to the amount of chemical bonding information that can be extracted from measured spectra.

Figure 7 shows the Raman spectra of 12MZ5A fibers depending on the sintering temperatures. At 800°C, the Raman spectra of the fibers have a typical disordered cubic bands with broad, poorly defined maxima at 149, 267, 323, 469, and 643 cm<sup>-1</sup>. As the sintering temperature is raised up to 1000°C, 14 Raman active bands of monoclinic phase are observed which are less than 18 Raman active modes predicted from the group theory.<sup>17,18</sup> There appear the characteristic tetragonal bands at 149 and 267 cm<sup>-1</sup> and from this fact we know that the tetragonal and monoclinic phase coexist. In contrast, at 1500°C, the intensities of monoclinic bands decrease considerably, while the cubic bands appear again.

The Raman spectra of 12MZ20A fibers are shown in figure 8. At 800°C, we observe a very broad continuum of Raman bands which is characteristic shape of disordered cubic phase. It is apparent from the shape of the Raman spectra of the disordered cubic phase that this solid solution behaves more like an amorphous than a crystalline compound.<sup>17</sup> At 1000°C, the Raman bands of tetragonal around 147, 267, 317, 467, and 645 cm<sup>-1</sup> develop more distinct and at 1200°C, tetragonal phase completely change to monoclinic. The doublet at 181 and 192 cm<sup>-1</sup> is the most characteristic of the monoclinic phase.

Figure 9 is IR and Raman spectra of Mg-PSZ/Al<sub>2</sub>O<sub>3</sub> fibers as a function of Al<sub>2</sub>O<sub>3</sub> content sintered at 1000°C. In the case of Al<sub>2</sub>O<sub>3</sub> free fibers, only monoclinic phase exists at 1000°C. When 5 mol% Al<sub>2</sub>O<sub>3</sub> is added to the 12MZ fibers, the Raman spectra reveal that both monoclinic and tetragonal bands coexist while only tetragonal bands appear with 20 mol% Al<sub>2</sub>O<sub>3</sub>. Fig. 9(b) shows the infrared spectra of Mg-PSZ/Al<sub>2</sub>O<sub>3</sub> fibers at 1000°C. The spectrum of the cubic phase of 12MZ20A show the appearance of very broad bands around 620 cm<sup>-1</sup>. The monoclinic spectra of Al<sub>2</sub>O<sub>3</sub> free MgO-ZrO<sub>2</sub> fibers are distinguished by an increase in number and sharpness of the bands. The 740 cm<sup>-1</sup> band is distinctive for this phase.<sup>18</sup>

## 3. The properties and microstructure of fibers

The DTA curves of the Mg-PSZ/Al<sub>2</sub>O<sub>3</sub> fibers containing 0, 5, 20 mol% Al<sub>2</sub>O<sub>3</sub> as shown in figure 10 represent the same tendency except the crystallization temperatures. The strong endothermic peak below 100°C is due to the

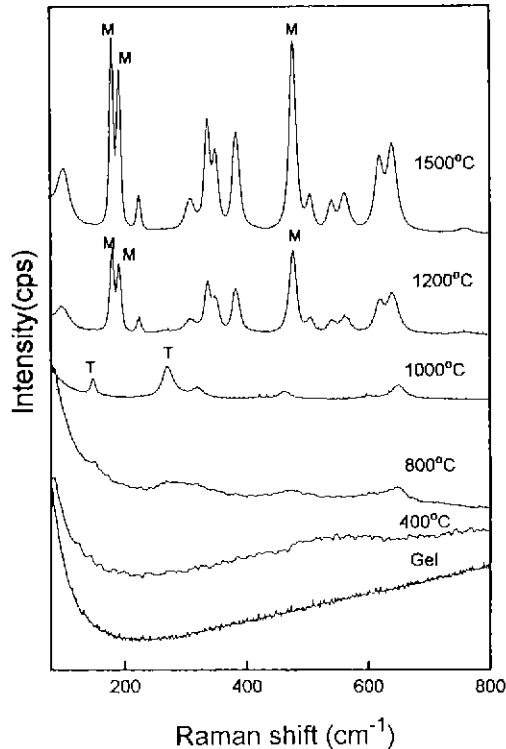
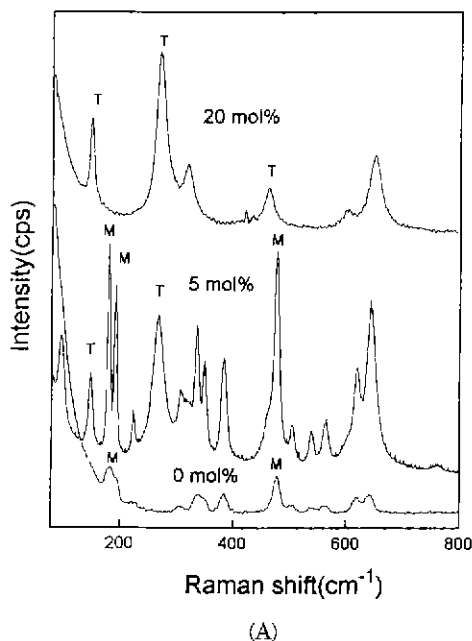
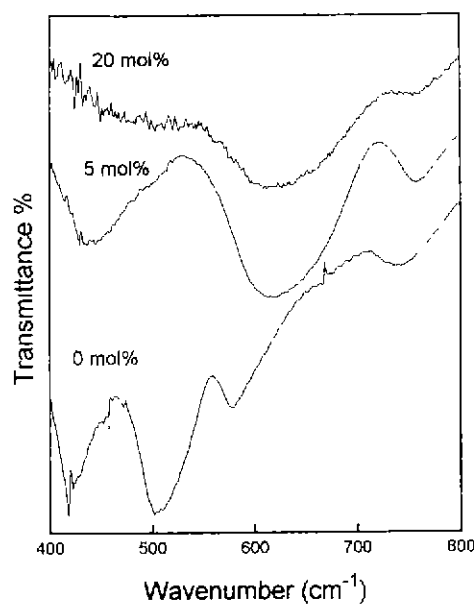


**Fig. 8.** Raman spectra of 12Mg-PSZ/20Al<sub>2</sub>O<sub>3</sub> (mol%) fibers sintered at different temperatures for 1 hr [M: Monoclinic, T: Tetragonal].



(A)



(B)

**Fig. 9.** Raman(A) and IR(B) spectra of 12Mg-PSZ/Al<sub>2</sub>O<sub>3</sub> fibers taken as a function of Al<sub>2</sub>O<sub>3</sub> amounts sintered at 1000°C for 1 hr [M: Monoclinic, T: Tetragonal].

dehydration and decomposition of alcohol and water of the gel fibers. After this, all fibers exhibit the exothermic peaks because of the decomposition of organic compounds until 300°C. The other feature of these curves is an exothermic peak in the range 400 to 600°C. The Al<sub>2</sub>O<sub>3</sub> free 12MZ fibers appear to transform into crystallized ZrO<sub>2</sub> between 400 and 500°C, while the transformation temperature into crystallized ZrO<sub>2</sub> depending upon the dopant Al<sub>2</sub>O<sub>3</sub> concentration shifts to 500°C and 600°C, respectively.

Figure 11 represents typical SEM photographs of 12MZ5A fibers as a function of sintering temperature. The hand-drawn fibers have various diameters and shape in cross-section. The diameter of prepared fibers is around 10~50 μm. In Figs. 11(A) and (B), the surface of 12MZ5A fiber remains very smooth and at 1500°C, the surface of fiber develops large grains with pores between them.

We investigated the microstructural variation of Mg-PSZ/Al<sub>2</sub>O<sub>3</sub> fibers depending on the amount of Al<sub>2</sub>O<sub>3</sub> at 1500°C (figure 12). Al<sub>2</sub>O<sub>3</sub> free 12MZ fibers in Fig. 12(A) and (B) consist of large grains and many pores with average grain size of 2 μm. The grain size was estimated by the equation of Wurst et al.<sup>19</sup> The addition of Al<sub>2</sub>O<sub>3</sub> suppresses the ZrO<sub>2</sub> grain growth. The SEM photographs of the fibers with 5 mol% Al<sub>2</sub>O<sub>3</sub> reveal that the average grain size of 0.59 μm while the grain size of 12MZ20A decreased more to 0.39 μm as shown in Figs. 12(E) and (F). Thus, in the present investigation, we observe the fact that Al<sub>2</sub>O<sub>3</sub> has a dramatic effect in reducing the ZrO<sub>2</sub> grain size from 2 μm to 0.39 μm at 1500°C.

As can be seen in figures 13, 14 and 15, tensile strength

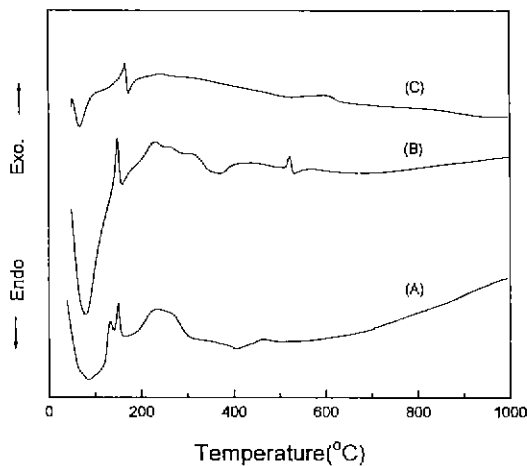


**Fig. 10.** DT analysis of 12Mg-PSZ/ $\text{Al}_2\text{O}_3$  fibers containing 0 mol%(A), 5 mol%(B), and 20 mol%(C)  $\text{Al}_2\text{O}_3$

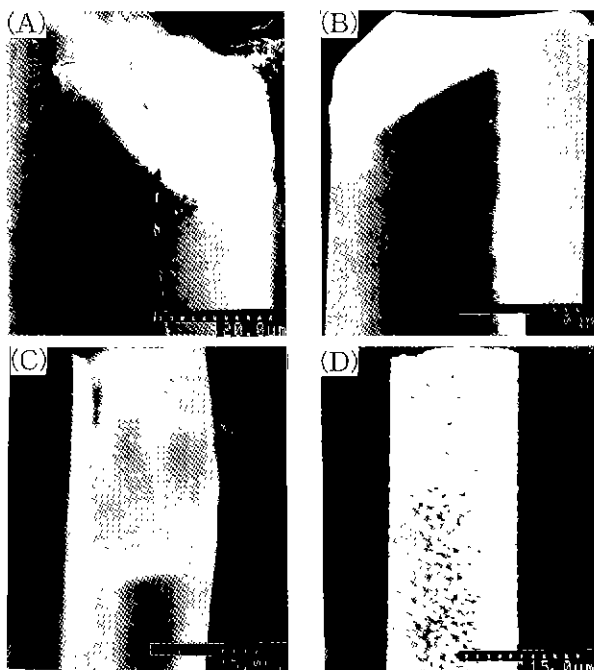


**Fig. 11.** SEM photographs 12Mg-PSZ/5 $\text{Al}_2\text{O}_3$ (mol%) fibers taken as a function of sintering temperatures: gel(A), 800°C (B), 1000°C(C), and 1500°C(D).

data are scattered, which may be caused by the differences in fiber diameter and shape in cross-section. In the previous study,<sup>9</sup> the average tensile strength of  $\text{Al}_2\text{O}_3$  free 12MZ fibers at 800°C was reported to have a value of 4 GPa at diameter of 20~30  $\mu\text{m}$ , while that of 1000°C-sintered fibers decreases to 0.7 GPa at the same diameter range. The average tensile strength of 12MZ5A fibers at 800°C is about 1.2 GPa at diameter of 10~20  $\mu\text{m}$  and 0.9 GPa at diameter of 20~30  $\mu\text{m}$ . The 1000°C-sintered fibers have higher tensile strengths than those of 800°C-sintered fibers and they are about 1.2 GPa at diameter of 20~30  $\mu\text{m}$ . The tensile strength of the fibers

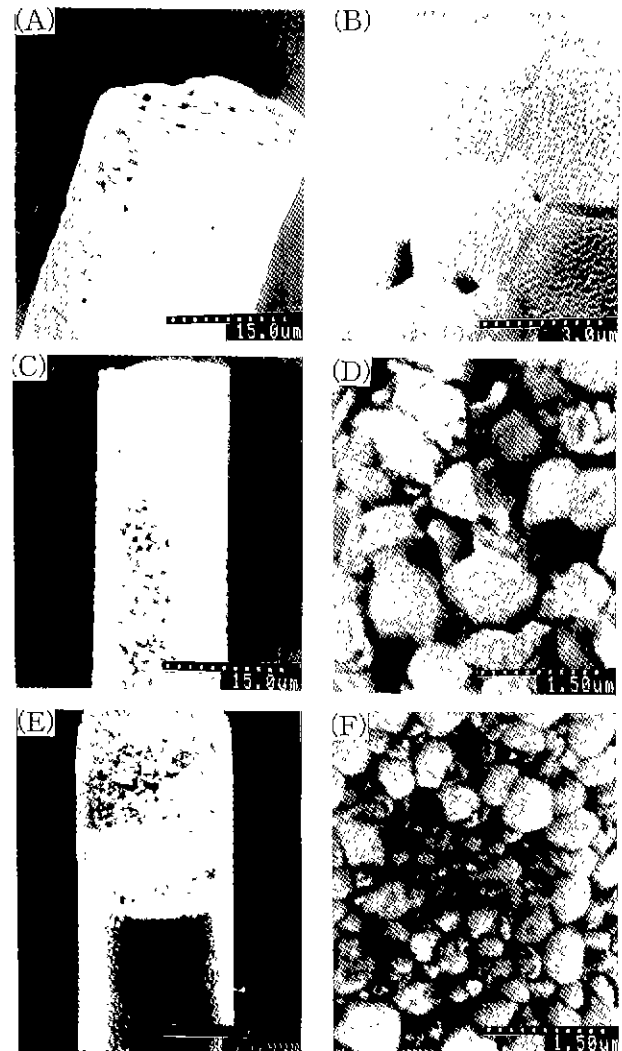


**Fig. 12.** SEM photographs of surface of 12Mg-PSZ(A)(B), 12Mg-PSZ/5 $\text{Al}_2\text{O}_3$ (C)(D), and 12Mg-PSZ/20 $\text{Al}_2\text{O}_3$ (E)(F) (mol%) fibers sintered at 1500°C for 1 hr.

containing 5 mol%  $\text{Al}_2\text{O}_3$  was found to have a higher value than that of the  $\text{Al}_2\text{O}_3$  free 12MZ fibers at 1000°C. Lange<sup>10</sup> reported that, in the PSZ/ $\text{Al}_2\text{O}_3$  systems, existence of cubic  $\text{ZrO}_2$  in the matrix lowers the fracture toughness as a consequence of residual stresses associated with the negative differential thermal expansion and shrinkage of the cubic  $\text{ZrO}_2$  with respect to the  $\text{Al}_2\text{O}_3$ . Therefore, we suppose that a considerable decrease in the tensile strength of 800°C-sintered 12MZ5A fibers is due to the existence of cubic phase in 12MZ5A fibers, as shown in the results of XRD and Raman spectroscopy.

For the 1000°C-sintered 12MZ20A fibers, the average tensile strength is about 0.6 GPa at diameter of 10~20  $\mu\text{m}$  and 0.3 GPa at diameter of 20~30  $\mu\text{m}$ , which exhibits the lower tensile strength than those of the 1000°C-sintered 12MZ5A fibers (figure 15). These results indicate that the existence of spinel in grain boundaries

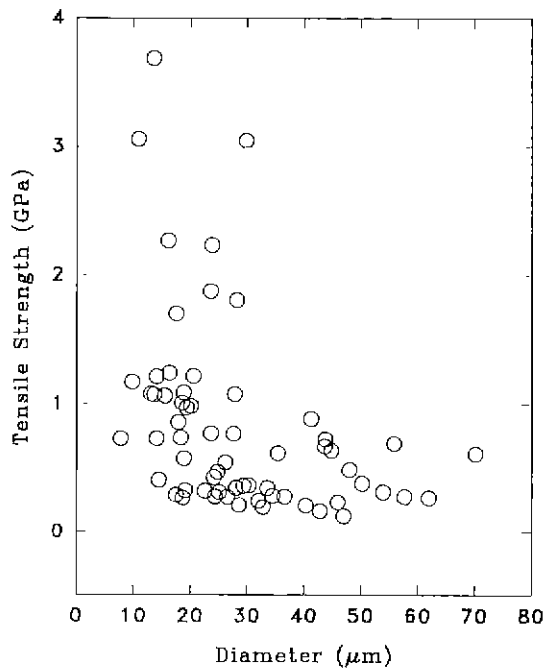


**Fig. 13.** Tensile strength of 12Mg-PSZ/5Al<sub>2</sub>O<sub>3</sub> (mol%) fibers sintered at 800°C for 1 hr.

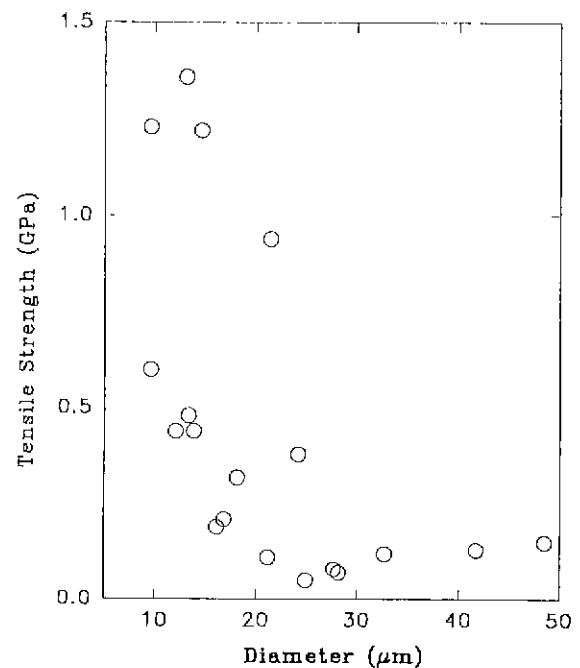


**Fig. 15.** Tensile strength of 12Mg-PSZ/20Al<sub>2</sub>O<sub>3</sub> (mol%) fibers sintered at 1000°C for 1 hr.

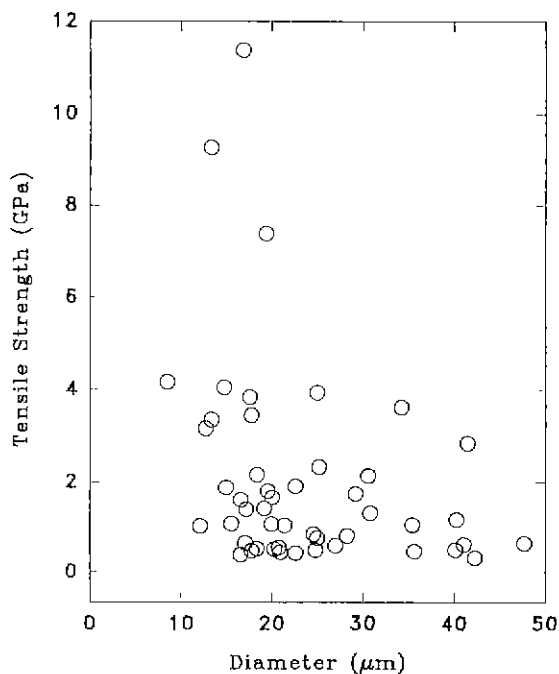


**Fig. 14.** Tensile strength of 12Mg-PSZ/5Al<sub>2</sub>O<sub>3</sub> (mol%) fibers sintered at 1000°C for 1 hr.

has a bad effects on the fiber tensile strength.

#### IV. Conclusions

Mg-PSZ/Al<sub>2</sub>O<sub>3</sub> fibers containing Al<sub>2</sub>O<sub>3</sub> of 5-20 mol% have been prepared by the sol-gel method. The conv-

ersion process of gel to oxide fibers at various sintering temperature and the phase transformation of fibers with different Al<sub>2</sub>O<sub>3</sub> content were compared with one another. The following results were obtained.

1. Mg-PSZ/Al<sub>2</sub>O<sub>3</sub> fibers were hand-drawn from the proper concentrated sol solutions and the prepared fibers have a diameter of 10 to 50 μm.

2. From the results of XRD and vibrational spectra, the phase transformation of Mg-PSZ/Al<sub>2</sub>O<sub>3</sub> fibers shows the following paths:

At 5 mol% Al<sub>2</sub>O<sub>3</sub>; amorphous → metastable cubic  
→ monoclinic+tetragonal → monoclinic  
→ cubic+monoclinic.

At 20 mol% Al<sub>2</sub>O<sub>3</sub>; amorphous → metastable cubic  
→ tetragonal+monoclinic  
→ monoclinic.

The crystalline spinel(MgAl<sub>2</sub>O<sub>4</sub>) start to appear at 1000°C and remains until 1500°C in both 12MZ5A and 12MZ20A samples.

3. The addition of Al<sub>2</sub>O<sub>3</sub> has a great influence on the retardation of ZrO<sub>2</sub> grain growth.

4. The average tensile strength of 12MZ5A fibers at 800°C is about 1.2 GPa at a diameter of 10-20 μm and 0.9 GPa at a diameter of 20-30 μm. The 1000°C-sintered fibers have higher tensile strengths than those of 800°C-sintered fibers and they are about 1.2 GPa at a diameter of 20-30 μm.

#### Acknowledgment

The financial support of this work from The Korea Research Foundation is gratefully acknowledged.



## References

1. C. Sakurai, T. Fukui, and M. Okuyama, "Hydrolysis Method for Preparing Zirconia Fibers," *J. Am. Ceram. Soc. Bull.*, **70**[4], 673 (1991).
2. E. Leory, C. Robin-Brosse, and J. P. Torre, "Fabrication of Zirconia Fibers from Sol-Gel," pp. 219-231 in *Ultrastructural Processing of Ceramics, Glasses and Composites*, Ed. by L. L. Hench and D. R. Ulrich, John-Wiley and Sons, NY (1984).
3. M. Kokubo, Y. Teranish, and T. Maki, "Preparation of Amorphous  $ZrO_2$  Fibers by Unidirectional Freezing of Gel," *J. Non-Cryst. Solids*, **56**, 411 (1983).
4. K. Kamiya, T. Yoko, K. Tanaka, and H. Itoh, "Preparation of Fibrous  $ZrO_2$  and  $CaO-ZrO_2$  from Zirconium Alkoxide by Sol-Gel Method," *Yogyo Kyokai-Shu*, **92**[12], 1157 (1987).
5. I. N. Yermolenko, T. M. Ulyanova, P. A. Vityaz, and I. L. Fyodorova, "Structure of Stabilized Zirconium Dioxide Fibers," pp. 367-375 in *Zirconia'88*, Ed. by S. Meriani and C. Palmonari, Elsevier Applied Science (1989).
6. S. Kim, S. S. Kim, and W. C. LaCourse, " $ZrO_2$  Ceramic Fiber Fabrication by Sol-Gel Processing," *J. Korean Ceram. Soc.*, **27**[6], 824 (1990).
7. K. Kamiya, K. Takahashi, T. Maeda, H. Nasu, and T. Yoko, "Sol-Gel Derived  $CaO$ - and  $CeO_2$ -Stabilized  $ZrO_2$  Fibers-Conversion Process of Gel to Oxide and Tensile Strength," *J. Eur. Ceram. Soc.*, **7**, 295 (1991).
8. C. M. Whang, and H. T. Eun, "Preparation of  $MgO-ZrO_2$  Fibers by Sol-Gel Method and Their Characterization," *J. Korean Ceram. Soc.*, **31**[10], 1147 (1994).
9. T. Yogo, S. Kodame, and H. Iwahara, "Synthesis of Polycrystalline Alumina-Zirconia Fiber Using Chelated Aluminum-Zirconium Precursor," *J. Mater. Sci.*, **28**, 105 (1993).
10. K. R. Venkatachari, L. T. Moeti, M. D. Sacks, and J. H. Simmons, "Preparation of Mullite-Based Fibers by Sol-Gel Processing," *Ceram. Eng. Sci. Proc.*, **11**[9-10], 1521 (1990).
11. K. Tsukuma, K. Ueda, K. Matsushita, and M. Shimada, "High-Temperature Strength and Fracture Toughness of  $Y_2O_3$ -Partially-Stabilized  $ZrO_2/Al_2O_3$  Composites," *J. Am. Ceram. Soc.*, **68**[2], c-56-c-58 (1985).
12. K. Tsukuma, and T. Takahata, "Mechanical Property and Microstructure of TZP and TZP/ $Al_2O_3$  Composites," pp. 123-35 in *Advanced Structural Ceramics*, Ed. by P.F. Becher, M.W. Swain, and S. Somiya, MRS, Pittsburgh, PA, 1987.
13. S. Sim, A. Morrane, and D. E. Clark, "Processing and Microstructure of Y-TZP/ $Al_2O_3$  Fiber," *Ceram. Eng. Sci. Proc.*, **11**[9-10], 1712 (1990).
14. T. Kosmac, D. Kolar, and M. Trontelj, "Diffusion Processes and Solid-State Reactions in the Systems  $Al_2O_3-ZrO_2$  (Stabilizing Oxide)( $Y_2O_3$ ,  $CaO$ ,  $MgO$ )," pp. 546-552 in *Advances in Ceramics, in Science and Technology of Zirconia II*, Ed. by N. Claussen, M. Ruhle, and A.H. Heuer, Am. Ceram. Soc., 1984.
15. P. Kundu, D. Pal, and Suchitra Sen, "Preparation and Thermal Evolution of Sol-Gel Derived Transparent  $ZrO_2$  and  $MgO-ZrO_2$  Gel Monolith," *J. Mater. Sci.*, **23**, 1539 (1988).
16. T. Y. Tseng, C. C. Lin, and J. T. Liaw, "Phase Transformations of Gel-Derived Magnesia Partially Stabilized Zirconias," *J. Mater. Sci.*, **22**, 963 (1987).
17. V. G. Keramidias, and W. B. White, "Raman Scattering Study of the Crystallization and Phase Transformations of  $ZrO_2$ ," *J. Am. Ceram. Soc.*, **57**[1], 22 (1974).
18. C. M. Phillippi, and K. S. Mazdhyasni, "Infrared and Raman Spectra of Zirconia Polymorphs," *J. Am. Ceram. Soc.*, **54**[5], 254 (1971).
19. J. C. Wurst, and J. A. Nelson, "Lineal Intercept Technique for Measuring Grain Size in Two-Phase Polycrystalline Ceramics," *J. Am. Ceram. Soc.*, **55**[2], 109 (1972).
20. F. F. Lange, "Transformation Toughening," *J. Mater. Sci.*, **17**, 225(1982).